Effects of intrauterine devices on proteins in the uterine lavage fluid of mares

Alamo, Maria Montserrat Rivera del

2021-04-15

Alamo , M M R D , Katila , T , Palviainen , M & Reilas , T 2021 , ' Effects of intrauterine devices on proteins in the uterine lavage fluid of mares ' , Theriogenology , vol. 165 , pp. 1-9 . https://doi.org/10.1016/j.theriogenology.2021.02.001

http://hdl.handle.net/10138/339800
https://doi.org/10.1016/j.theriogenology.2021.02.001

Title

Effects of intrauterine devices on proteins in the uterine lavage fluid of mares

Running title

Proteins in equine uterine lavage fluid

MM Rivera del Alamo[1], T Katila [2], M Palviainen[3], T Reilas[4]

[1]Unit of Reproduction, Faculty of Veterinary Medicine, Travessera dels Turons s/n Autonomous University of Barcelona, 08193 Bellaterra, Spain. E-mail address: mariamontserrat.rivera@uab.cat

[2]Department of Production Animal Medicine, Faculty of Veterinary Medicine, University of Helsinki, Finland. E-mail address: terttu.katila@helsinki.fi

[3]Department of Equine and Small Animal Medicine, Faculty of Veterinary Medicine, University of Helsinki, Finland. E-mail address: mari.palviainen@helsinki.fi

[4]Natural Resources Institute Finland (Luke), Jokioinen, Finland. E-mail address: tiina.reilas@luke.fi

***Corresponding author**

Maria Montserrat Rivera del Alamo, Department of Animal Medicine and Surgery, Faculty of Veterinary Medicine, Autonomous University of Barcelona, Bellaterra (Cerdanyola del Vallès), E-08193 Spain. Tel.: +34 935811045, Fax.: +34 935812006, e-mail address: mariamontserrat.rivera@uab.cat

Abstract

Intrauterine devices block luteolysis in cyclic mares, but the underlying mechanism is unknown. To clarify the mechanisms, the protein profile of the endometrial secretome was analyzed using two-dimensional difference gel electrophoresis (2D-DIGE). Twenty-seven mares were classified according to whether they were inseminated (AI) or had an intrauterine device (IUD), a water-filled plastic sphere, inserted into the uterus on Day 3 after ovulation. Uterine lavage fluids were collected on Day 15 from pregnant inseminated mares (AI-P; n = 8), non-pregnant inseminated mares (AI-N; n = 4), and mares with IUD (n = 15). The IUD group was further divided into prolonged (IUD-P; n = 7) and normal luteal phase (IUD-N; n = 8) groups on the basis of ultrasound examinations, serum levels of progesterone and PGFM on Days 14 and 15, and COX-2 results on Day 15. Four mares from each group were selected for the 2D-DIGE analyses. Ten proteins had significantly different abundance among the groups, nine of the proteins were identified. Malate dehydrogenase 1, increased sodium tolerance 1, aldehyde dehydrogenase 1A1, prostaglandin reductase 1, albumin and hemoglobin were highest in pregnant mares; T-complex protein 1 was highest in non-pregnant mares; and annexin A1 and 6-phosphogluconolactonase were highest in IUD mares. The results suggest that the mechanism behind the intrauterine devices is likely related to inflammation.

Key words: mare; 2D-DIGE; endometrial proteins; intrauterine device; pregnancy

Introduction

Intrauterine devices (IUDs) are used as a method to suppress estrus behavior in competing mares. The underlying mechanisms of inducing prolonged luteal phases have not been completely elucidated, but embryo simulation by contact with the endometrial wall and endometrial inflammation have been suggested [1-3].

The hypothesis of embryo simulation was initially proposed for three reasons. First, the size of the plastic device is identical to that of an embryo during the time frame of maternal recognition of pregnancy. Secondly, the device can move slightly in the uterine lumen [2], and embryo movement is mandatory for blocking luteolysis [4] during maternal recognition of pregnancy in the mare. Thirdly, the device is in contact with the endometrium, similar to an embryo.

It has been shown that embryo contact with the endometrium – which is enhanced by moving around in the uterus – is involved in the inhibition of luteolysis by attenuating the secretion of $PGF_{2\alpha}$. Specifically, contact of the embryo with the endometrium triggers mechanotransduction mechanisms that induce changes in endometrial protein abundance during pregnancy [5].

Although inflammation is a logical explanation for the effectiveness of IUDs, the evidence for this is not consistent. After IUD use for one year in wild horses, all mares had chronic endometritis at the time of IUD removal [6]. In previous IUD experiments in mares, non-echogenic intrauterine fluid was reported during IUD treatment [1,2], but it was not associated with inflammation in endometrial biopsy samples obtained after IUD removal [1,2,7,8]. It is possible that the mares had previous inflammation which was resolved by the time the biopsies were taken, or at least acute inflammation had already been resolved and turned chronic. It is also possible that the diagnostic methods used to detect inflammation in the previous studies were not sensitive enough.

It has been shown that IUDs suppress cyclooxygenase-2 (COX-2) [3], leading to the inhibition of $PGF_{2\alpha}$ release and maintenance of the corpus luteum (CL) [2]. However, the events preceding COX-2 inhibition remain unknown. We do not know how the presence of an IUD is mediated to the endometrium to suppress COX-2. Likewise, differences between mares in the efficacy of the devices to prolong luteal function have yet to be elucidated. However, adequate perfusion and drainage of the endometrium seem to increase the efficacy of the devices to inhibit luteolysis [8].

Uteroferrin staining was increased in endometrial biopsies of mares in which the presence of an IUD resulted in prolonged CL function [8]. This may indicate inflammation, but it also shows that the presence of a device in the uterus induces changes in the composition of endometrial secretions. Other uterine proteins, such as annexin 2, eukaryotic initiation factor 4A1, protein disulphide isomerase, superoxide dismutase and transketolase have been described to be involved in processes of endometrial inflammation in bovine species [9].

During early pregnancy, endometrial secretions – mostly consisting of proteins – are essential. They play a crucial role in implantation and development of the conceptus [10]. Changes in the composition across the estrus cycle are thought to occur to provide the most appropriate environment in the different events of a successful pregnancy [10].

The aim was to gain new insights into the mechanisms by which IUDs prevent luteolysis. Our hypothesis was that the protein composition in endometrial secretions on Day 15 after ovulation differs between pregnant, non-pregnant and IUD mares. For this purpose, a proteomic study using two-dimensional difference gel electrophoresis (2D-DIGE) analysis [11], which allows to compare simultaneously multiple protein samples in the same gel thus reducing the experimental and analytical time, was performed on uterine

lavage fluids collected previously [3] from pregnant and non-pregnant mares, and from mares with an IUD exhibiting a prolonged or normal luteal phase.

Material and methods

Animals

Twenty-seven mares (Finnhorses and four warmbloods) from Equine College Ypäjä and MTT Agrifood Research Ypäjä (Finland) were initially included in the present study. The mean age was 9.6 years (ranging from 4 to 17 years); live weights ranged from 500 to 590 kg. The mares had foaled 0 to 7 times, had no history of reproductive failure, and were clinically normal. They were ranked by age, number of foalings and breed, and then assigned alternately into two groups: the inseminated group (AI) (n=12; mean age 9 years; mean number of foalings 0.75) and the intrauterine device group (IUD) (n = 15; mean age 10.3 years; mean number of foalings 1). These groups were further divided into four sub-groups depending on the results of serum progesterone, COX-2 and ultrasound examination [2]: pregnant (AI-P; n = 8; mean age 6.1 years) and non-pregnant (AI-N; n = 4; mean age 14.8 years); prolonged (IUD-P; n = 7; mean age 9.3 years) and normal luteal phase (IUD-N; n = 8; mean age 10.8 years).

The permission for animal experimentation was granted by the provincial government of Southern Finland (number 1102101).

Experimental design

Experimental protocol is shown in Fig. 1. The mares included in the study were examined every other day by transrectal palpation and ultrasonography (SonoSite Vet 180 Plus with a 4 MHz linear array transducer; Sono Site Inc., Bothell, WA, USA). Once in early estrus,

116 the examinations were performed daily until ovulation was detected. The ovulation day
117 was assigned as Day 0.
118 When a ≥35-mm follicle was observed by ultrasound, an injection of 1500 IU of hCG
119 (Chorulon®, Intervet International B.V., Boxmeer, The Netherlands) was given to time
120 ovulation. The mares in the AI group were inseminated approximately 24 hours after hCG
121 administration with a proven stallion. In the IUD group, the device was inserted in the
122 uterus on Day 3 after ovulation using the double-glove technique [12]. The device was a
123 water-filled polypropylene ball, 20 mm in diameter [2].
124 Blood samples for progesterone were obtained on Days 0, 3, 5, 7, 9, 11, 13, 14, and 15
125 after ovulation and analyzed by means of the Spectria Progesterone radioimmunoassay
126 (RIA) kit (Orion Diagnostica, Espoo, Finland), using the 1270 Rackgamma counter
127 (Wallac Oy, Turku, Finland). The detection limit of the equipment was 0.7 nmol/L. Intra-
128 and inter-assay coefficients of variations for low, medium and high levels of progesterone
129 were 11.5%, 3.0% and 3.8% (intra-), and 7.8%, 5.1% and 4.8% (inter-) respectively. In
130 addition, serial blood samples were obtained to determine serum levels of 15-
131 ketodihydro-$PGF_{2\alpha}$ (PGFM) on Days 14 and 15 after ovulation, as previously described
132 [3] and analyzed according to Granström and Kindahl [13]. The detection limit of the
133 assay was 60 pmol/L. The inter- and intra-assay coefficients of variation were 11.7% and
134 6.6 respectively.
135 On Day 14, the mares were examined by transrectal palpation and ultrasonography to
136 determine the stage of the estrus cycle, the presence or absence of an embryo in the AI
137 mares, and the location of the device in the IUD mares.
138 On Day 15, 30 ml of warm (37ºC) phosphate buffered saline (PBS; pH 7.0) was infused
139 into the uterus via a Foley catheter, and the uterus was briefly massaged per rectum. After
140 5 min of equilibration, the fluid was allowed to drain into a sterile centrifuge tube [13].

The lavage fluid was kept on ice until centrifuged; after centrifugation, the supernatant was collected and stored at -80ºC until analyzed. Lavage fluid was used for protein analyses by 2-DIGE techniques [14].

2D-DIGE analysis

Animal selection for 2D-DIGE analysis

For 2D-DIGE analysis, four mares from each of the four groups were selected. The selection criterion for AI-N mares was the absence of an embryo, and for AI-P mares the presence of an embryo and high serum progesterone. In the IUD mares, serum progesterone and plasma PGFM concentrations, and endometrial COX-2 expression were used to determine a normal or prolonged luteal phase. PGFM concentrations of 60–100 pmol/L were defined as low, 101–200 pmol/L as intermediate, and >200 pmol/L as high. Thus, four mares with progesterone concentrations between 1–5 nmol/L on Day 15, two to five distinctive PGFM pulse releases (368–739 pmol/L), and positive expression for COX-2 in immunoblotting and immunohistochemistry were included in the normal luteal phase group (IUD-N), while four mares with progesterone concentrations between 14–26 nmol/L, mostly low PGFM values (60/64 values low, 3/64 intermediate, and one value of 256 pmol/L), and negative expression for COX-2 were included in the prolonged luteal phase group (IUD-P) [3]. Mean ages in AI-P, AI-N, IUD-P and IUD-N groups for 2D-DIGE analysis were 5.5, 14.8, 10.5 and 8.8 years, respectively. A workflow for the 2D-DIGE analysis of uterine lavage fluid is shown in Supplementary Fig. S1.

Sample preparation and CyDye labelling

Proteins from the uterine lavage samples were first treated with 0.1 U chondroitinase ABC and 0.1 U betaglucuronidase to remove glycans. Proteins were then precipitated

with trichloroacetic acid-acetone precipitation and solubilized in 50 µl of labelling buffer (7 M urea, 2 M thiourea, 4% cholamidopropyl[dimethylammoniol]-1-propanesulfonate hydrate (CHAPS), 30 mM Tris). Protein concentration was measured by using a 2D Quant Kit (GE Healthcare) following the manufacturer's instructions. The samples were then labelled with Cy2, Cy3 and Cy5 dyes (CyDye DIGE Fluor minimal dyes, GE Healthcare) according to the Ettan two-dimensional difference gel electrophoresis (DIGE) protocol (Supplementary Fig. S1). Briefly, 50 µg of protein from each sample was labelled with 400 pmol of the Cy3 and Cy5 dyes. An internal standard was established by combining 25 µg of each sample and labelled with Cy2 dye. The labelling reaction was incubated for 30 minutes on ice in the dark, and stopped by adding 1 mM lysine to the reaction following a 10-minute incubation period.

Two-dimensional gel electrophoresis

Labelled proteins were analyzed by DIGE as described earlier [15]. An immobilized pH gradient (IPG) strip (24 cm, pH 3–10, nonlinear, GE Healthcare) was used for isoelectric focusing. IPG strips were loaded with 150 µg of protein in total by using the cup-loading method. Isoelectric focusing was performed using IPGPhor (GE Healthcare) at 20°C as follows: 3 h at 150 V, 3 h at 300 V, linear ramping to 10 000 V and 10 000 V for 50 000 Vh with a maximum current of 75 µA per strip. After focusing, the isoelectric strips were prepared for the second-dimension gels by incubation in equilibrium buffer I (50 mM Tris pH 8.8, 6 M urea, 30% glycerol, 2% sodium dodecyl sulphate (SDS), 0.2% bromophenol blue, with added 10 mg/ml dithiothreitol (DTT)) solution for 15 minutes. This was followed by incubation in equilibrium buffer II (50 mM Tris pH 8.8, 6 M urea, 30% glycerol, 2% SDS, 0.2% bromophenol blue, supplemented with 25 mg/ml iodoacetamide) for another 15 minutes. The prepared IPG strips were then placed on 12% sodium dodecyl

sulphate (SDS) polyacrylamide gels (SDS-PAGE) and sealed with overlay agarose (Bio-Rad). Electrophoresis was initiated at 50 V for 30 minutes, followed by 300 V for 3 hours. The gels were scanned between low-fluorescence glass plates using an FLA-5100 laser scanner (Fujifilm) at wavelengths 473 (for Cy2), 532 (for Cy3), and 635 nm (Cy5) using voltages of 420, 410 and 400 V, respectively. After scanning, the gels were silver stained as previously described [16]. Each evaluated group had four biological replicates.

Image analysis and statistical processing of the data

The gel images were analyzed and statistically assessed using DeCyder 7.0 software (GE Healthcare). First, the gels were automatically analyzed using the batch processor function to normalize the Cy2, Cy3 and Cy5 images from each gel. Spot volumes were calculated based on the intensity of the signal of each spot (Cy3 or Cy5), and compared to Cy2 volumes (internal standard) to correct the inter-gel variations. In the biological variation module, the Cy2 images of all eight gels were matched and the spot volumes were compared. Approximately 7000 separate spots were detected on each gel. Protein spots demonstrating at least a 1.5-fold difference in average spot volume ratios between groups in all biological replicates were selected and analyzed with mass spectrometry. Spot volume ratios were calculated using one-way ANOVA, with a *P*-value of less than 0.05 as the selection criteria.

Protein identification

Protein spots of interest were manually cut from the gel and digested in-gel using trypsin (Trypsin Gold, Mass spectrometry grade, Promega) as earlier described [17,18]. The samples were first concentrated and desalted on a C_{18} trap column (PROTECOL, SGE Analytical Science, Griesham, Germany) followed by peptide separation on a PepMap

100 C_{18} analytical column (LC Packings, Sunnyvale, CA). MS/MS of peptides was performed on a hybrid quadruple/TOF mass spectrometer with Nanospray II source (QSTAR Elite, applied Biosystems, Foster City, CA). The identification of proteins was performed using the local Mascot version 2.2 (matrix science, London, UK) against the in-house database. The search criteria included digestion with one missed cleavage allowed, as a fixed modification carbamidomethyl modification of cysteine and as a variable modification oxidation of methionine.

Verification of identified proteins

All individual samples included in 2D-DIGE analysis from each group were pooled and used for validation by Western blot analysis (Fig. 4). SDS-PAGE was carried out in 12% polyacrylamide gels using a vertical slab gel apparatus under non-reducing conditions (Bio-Rad TetraCell) as described previously [19]. A 20-µl aliquot of each pooled sample was loaded to the gel, and proteins were separated by electrophoresis at 100 V for 3 h. Proteins were transferred to a PVDF membrane (Immobilon, Amersham) using a semidry blotting apparatus (Bio-Rad). Membranes were blocked for 1 hour using 5% bovine serum albumin in Tris-buffered saline containing 0.1% Tween-20 (TBST), and probed using polyclonal anti-6-phosphogluconolactonase (6PGL C14200, Assay Biotech, 1:1000), monoclonal anti-increased sodium tolerance 1 (IST1, clone C7, antibodies-online, 1:1000), polyclonal anti-prostaglandin reductase 1 (PTGR1, C16862, Assay Biotech, 1:1000), polyclonal anti-aldehyde dehydrogenase 1A1 (ALDH1A1, bs-6509R, antibodies-online, 1:500), polyclonal anti-malate dehydrogenase 1 (MDH1, ABIN2783316, antibodies-online, 1:500) or polyclonal anti-annexin A1 (ANXA1, bs-1562R, antibodies-online, 1:1000), in TBST at 4°C, respectively. The signals were detected using horseradish peroxidase-conjugated secondary anti-rabbit (sc-2004, Santa

241 Cruz, 1:2000) or anti-mouse (P0447, Daco, 1:1000) and SupserSignal West Dura
242 Chemiluminescent Substrate (Thermo Scientific), and the intensities were quantified with
243 a chemiluminescent image analyzer LAS3000 (Fujifilm). There was no commercial
244 antibody available against the T-complex protein 1 subunit theta (TCP1) and therefore
245 the biological verification of the protein was not conducted.
246
247 ***Gene ontology analysis***
248 To gain further insight into the role of these proteins, gene ontology (GO) analysis was
249 conducted with the FunRich analysis tool [20]. Proteins were mapped for molecular
250 function, cellular component and biological process of GO terms.
251
252 **Results**
253 ***2D-DIGE***
254 In the 2D-DIGE analysis, approximately 7000 different spots were visualized in gels. Ten
255 of these spots had different ($P < 0.05$) abundance in the uterine lavage fluids between AI-
256 P mares and the other groups (Fig. 2). Nine of the ten spots were identified by LC-
257 MS/MS: in addition to albumin and hemoglobin, TCP1, 6PGL, IST1, PTGR1,
258 ALDH1A1, MDH1, and ANXA1 (Table 1).
259 Of the total ten proteins, seven were highest in the AI-P group, one in the AI-N group,
260 one in the IUD-N group, and one in the IUD-P group (Fig. 3; Table 2).
261 Annexin A1 was up-regulated in IUD mares, with the IUD-P mares showing the highest
262 values, while it was down-regulated in pregnant mares (Table 2; Fig. 3). In contrast, IST1,
263 ALDH1A1, PTGR1, MDH1, albumin and hemoglobin, as well as the non-identified
264 protein, were up-regulated in pregnant mares, while down-regulated in non-pregnant

mares. In addition to ANXA1, TCP1 and 6PGL were down-regulated in pregnant mares (Fig. 3).

The average ratio of 2D-DIGE expression of the different identified proteins was calculated by using pregnant mares as the control group. The average ratio between non-pregnant and pregnant mares was significantly different in all identified proteins. The average ratio between IUD-N and pregnant mares was significantly different in TCP-1, ANXA1 and 6PGL. Finally, the average ratio between the IUD-P and pregnant mares was significantly different in TCP-1, IST1, MDH1, and ANXA1 (Table 2).

All identified proteins were within the expected size and pI ranges in the 2D analysis. Western blot results verified the identification of the proteins (Fig. 4).

GO annotations

The top ten GO terms enriched for the cellular component, molecular function and biological process of all identified proteins are shown in Fig. 5. Statistically significant GO terms are listed in Supplementary Table S1. The most prominent cellular component GO terms were extrinsic component of endosome membrane (GO:0031313), extrinsic component of external side of plasma membrane (GO:0031232) and phagocytic cup (GO:0001891). For the molecular function, the most enriched GO terms were phospholipase A2 inhibitor activity (GO:0019834), retinal dehydrogenase activity (GO:0001758), and calcium-dependent phospholipid binding (GO:0005544). The proteins were enriched in 56 biological process GO terms, of which the most prominent ones were regulation of interleukin-1 production (GO:0032612), negative regulation of T-helper 2 cell differentiation (GO:0045629), and positive regulation of T-helper 1 cell differentiation (GO:0045627).

Discussion

Pregnant mares had the highest endometrial levels of MDH1, IST1, ALDH1A1 and PTGR1. GO analysis of molecular function of these proteins revealed significant enrichment in oxidoreductases: oxidases and dehydrogenases.

MDH1 is a cytosolic protein involved in the Krebs cycle and NADH metabolic processes that transform malate into oxaloacetate. Literature on the role of MDH1 in female reproduction is scarce. Higher endometrial levels of MDH1 have been observed in pregnant mares compared with cyclic mares on day 13 after ovulation [21]. This protein is crucial for the proper development of the embryo in mice [22] and sows [23]. Considering that the embryo is a highly replicating structure, it can be hypothesized that MDH1 might be involved in fulfilling the glucose, glutamine and oxidative phosphorylation demands of the equine embryo.

IST1 is a member of the endosomal sorting complexes required for transport (ESCRT), specifically ESCRT-III [24,25]. The GO analysis revealed that the microtubule organizing center was the most enriched component for IST1. It has been shown that the depletion of IST1 inhibits cellular division [26], suggesting that IST1 is involved in the cytokinesis phase of cellular reproduction. It is hence possible that the presence of an embryo induces the production and/or release of IST1 in the uterine lumen. Furthermore, it can be hypothesized that the higher levels of IST1 in the uterine lumen may be involved in the cellular multiplication of the growing embryo. According to the literature, this is the first time that this protein is described in equine uterine fluid.

ALDH1A1 is a cytosolic enzyme that metabolizes retinal to retinoic acid [27]. Its molecular functions include retinal, aldehyde, and benzaldehyde dehydrogenase activity, and it participates in retinoid and retinol metabolic processes. Retinoid acid is crucial for the proper development of the embryo. Both deficiency and excess of this molecule are

315 linked with teratogenic abnormalities during embryogenesis [28-30]. Retinoic acid is
316 involved in the processes of neurogenesis, cardiogenesis and body axis extension, as well
317 as in the development of the forelimb buds, foregut and eye [27]. Thus, the high
318 expression of ALDH1A1 in the uterine lumen of pregnant mares can be explained by the
319 presence of the developing embryo.
320 Since these proteins, MDH1, IST1, and ALDH1A1, are all involved in either cellular
321 replication, embryogenesis or metabolic pathways, it seems logical to assume they also
322 play a role in conceptus development.
323 PTGR1 is a cytosolic prostaglandin reductase involved in PG-metabolism. As it has been
324 stated above, PTGR1 was up-regulated in pregnant mares, which is in agreement with a
325 previous study [21]. Its molecular functions include 2-alkenal reductase [NAD(P)] with
326 15-oxo -PGE1, -PGE2 or -PGE2-α as substrates, 13-prostaglandin reductase, which
327 produces the transient PGF metabolite, and 15-oxoprostaglandin 13-oxidase activity. The
328 latter enzyme initiates metabolic inactivation of leukotriene B_4 (LTB_4) [31], which is
329 known to be involved in many inflammatory processes [32] including neutrophil
330 recruitment [33]. During the period of implantation, the human endometrium shows signs
331 of inflammatory processes, such as the presence of interleukin 1 (IL1), IL6, IL8, leukemia
332 inhibitory factor and tumor necrosis factor [34], demonstrating that some steps of
333 inflammatory pathways are necessary for the proper establishment of pregnancy.
334 However, some important differences have been observed between implantation
335 inflammation and inflammation in response to disease or injury. The most outlined
336 difference is the lack of neutrophils during implantation [35]. The present results suggest
337 that the inhibition of LTB_4 by PTGR1 might be involved either in the maternal
338 recognition of pregnancy or pregnancy maintenance.

ANXA1 and 6PGL were up-regulated in IUD-P and IUD-N groups. GO analysis of these proteins shows that they are involved in phospholipase A2 (PLA2) inhibitor activity, calcium-dependent phospholipid binding, protein binding, bridging, calcium ion binding, and structural molecule activity. All the ten mostly enriched biological processes and cellular components were associated with annexin A1, as well as the most important molecular function, PLA2 inhibitor activity. Hence, annexin A1 appears to be the most significant component of endometrial secretomics at the time of sampling in our study.

Annexin A1 is a calcium/phospholipid-binding protein that has several functions including promotion of membrane fusion, involvement in exocytosis, and regulation of PLA2 activity [36]. Phospholipase A2 induces the release of arachidonic acid, which is the precursor molecule of prostaglandins, through the action of cyclooxygenases. In the present study, Annexin A1 was down-regulated in pregnant mares. However, previous studies have shown that this specific protein is up-regulated in the intrauterine fluid during early pregnancy in sows [37], sheep [38] and mares [21], linking its action to maternal recognition of pregnancy. The main difference between the studies performed in mares is the different sampling time. In the present study, the mares were sampled on Day 15 after ovulation, while in the study of Smits et al. [21] they were sampled on Day 13. Since maternal recognition of pregnancy in the mare occurs between days 12 and 14 after ovulation [21], it is possible that ANXA1 might be involved in the process of preventing luteolysis by inhibition of PLA2. Once maternal recognition has taken place, ANXA1 levels might decrease again similar to the present results. This hypothesis is sustained by an earlier study [39], which demonstrated that proteomic expression of uterine fluid in pregnant heifers varies depending on the day of pregnancy.

Annexin A1, an anti-inflammatory mediator, may be induced by glucocorticoids in inflammatory cells, and shares with these drugs many anti-inflammatory effects. It is

364 important in the resolution of inflammation and is therefore induced in inflammatory
365 conditions [40]. Annexin A1 inhibits inducible nitric oxide synthetase (iNOS) in
366 macrophages and COX-2 in activated microglia. The inhibition of iNOS expression may
367 be caused by the stimulation of IL-10 release induced by annexin A1 in macrophages
368 [40]. Like glucocorticoids, annexin A1 exerts profound inhibitory effects on both
369 neutrophil and monocyte migration in inflammation. Annexin A1 has been recently
370 identified as one of the signals on apoptotic cells to be recognized and ingested by
371 phagocytes, thus it may contribute to the safe post-apoptotic clearance of dead cells [41].
372 Since ANXA1 had the highest abundance in IUD mares, it seems likely that the presence
373 of IUDs in the uterine lumen provokes inflammation, which in turn induces annexin A1
374 release contributing to the inhibition of luteolysis. The highest abundance of annexin A1
375 was detected in IUD-P mares, which suggests that an intense inflammation may increase
376 the efficacy of the device.
377 6PGL is an intermediate enzyme in the pentose phosphate pathway (PPP) that transforms
378 6-phosphogluconolactone to 6-phosphogluconate [42]. During pregnancy – mainly
379 during implantation – glucose consumption is increased to meet ATP requirements [43],
380 and the PPP plays a key role to cover these necessities. In the present study, 6PGL showed
381 a lower expression in pregnant mares (AI-P) compared to non-pregnant mares (AI-N).
382 This result disagrees with that of Smits et al. [21] who observed higher concentrations of
383 6PGL in uterine fluid on day 13 of pregnancy in comparison with cyclic mares on the
384 same day after ovulation. Once again, a possible explanation for this difference could be
385 the fact that the mares were sampled on different days of pregnancy. Expression of 6PGL
386 was similar in IUD and non-pregnant mares. Thus, the presence of the device in the uterus
387 did not induce any change in the expression of 6PGL compatible with a pregnancy.

T-complex protein 1 subunit theta is a cytosolic protein that belongs to the T-complex protein 1 (TCP-1) chaperone family. It participates in the folding of protein complexes, [44,45] and is involved in cell growth, proliferation and apoptosis [46] and inflammation [47]. In the present study, pregnant mares showed the lowest expression of TCP-1, whereas AI-N mares had the highest expression.

Finally, hemoglobin and albumin were also present in higher abundance in intrauterine fluid samples from pregnant mares. The role of hemoglobin and albumin in intrauterine fluid is controversial. Since intrauterine fluid contains abundant blood proteins, some studies consider their presence as contamination [48]. However, some other studies have demonstrated the presence of hemoglobin in human endometrium and suggested a role during implantation [49,50]. Higher concentrations of hemoglobin in intrauterine fluid from pregnant mares have been previously described [21], which is in accordance with our results. However, further research is warranted to establish the possible role of hemoglobin in the pregnant mare. Uterine concentration of albumin is increased in acute iatrogenic endometritis in mares [51], and its presence has been reported both in pregnant and non-pregnant mares [52], but no role in normal early pregnancy has been described to date.

Given these results, it appears that the presence of an embryo or IUD induces changes in the protein composition of endometrial secretions on Day 15 after ovulation. In the study by Klohonatz et al. [5], the contact of the embryo/IUD with the endometrial wall induced the formation of adhesion molecules that are involved in mechanisms of mechano-transduction. The released adhesion molecules differed between embryos and IUDs However, unlike our results, Klohonatz et al. [5] found that the IUD did not block $PGF_{2\alpha}$ release. A possible explanation for this disagreement is the fact that the former study was performed *in vitro*, while ours was done *in vivo*.

Annexin A1 proved to be the most important protein in the endometrial secretomics in this study, as all major biological processes were due to annexin A1. Moreover, they were related to the regulation of inflammation or immune reactions: differentiation of T-cells, leukocyte migration, granulocyte chemotaxis, neutrophil apoptosis and interleukin production. The high levels of annexin A1 in IUD mares suggest that the IUD caused inflammation, which subsequently induced annexin A1 to down-regulate the inflammation. Since annexin A1 is a PLA2 inhibitor, it also prevented COX-2 and subsequent $PGF_{2\alpha}$ release. This is likely the mechanism by which IUDs block the luteolysis.

The present study has some limitations, such as the low number of mares in all groups, as well as the subgroup heterogeneity in terms of age. Another point to consider is the possibility of a delayed [53] or partial luteolysis [54], making Day 15 maybe too early for luteolysis to be completed in some non-pregnant mares.

The protein composition of endometrial secretions differed between pregnant and IUD-P mares, and Annexin A1, an inflammatory mediator, was up-regulated in IUD-mares. In conclusion, the results of the present study suggest that intrauterine devices cause endometrial inflammation which contributes to the inhibition of luteolysis.

Declaration of interest

The authors declare that no conflict of interest exists.

Funding

This work was supported by Finnish Veterinary Research Foundation and the Agència de Gestió d'Ajuts Universitaris i de Recerca (AGAUR).

Author contribution statement

All authors contributed to the planning of the study. Maria Montserrat Rivera del Alamo and Tiina Reilas carried out the animal experiments. Mari Palviainen performed the DIGE analysis and analyzed the data. Maria Montserrat Rivera del Alamo wrote the draft of the manuscript, and all authors contributed to the writing of the manuscript and approved it.

References

[1] Nie GJ, Johnson KE, Braden TD, Wenzel JGW. Use of an intra-uterine glass ball protocol to extend luteal function in mares. J Equine Vet Sci 2003;23:266-73.

[2] Rivera del Alamo MM, Reilas T, Kindahl H, Katila T. Mechanisms behind intrauterine device-induced luteal persistence in mares. Anim Reprod Sci 2008;107:94-106.

[3] Rivera del Alamo MM, Reilas T, Galvão A, Yeste M, Katila T. Cyclooxygenase-2 is inhibited in prolonged luteal maintenance induced by intrauterine devices in mares. Anim Reprod Sci 2018;199:93-103.

[4] Ginther OJ. Mobility of the early equine conceptus. Theriogenology 1983;19:603-11.

[5] Klohonatz KM, Nulton LC, Hess AM, Bouma GJ, Bruemmer JE. The role of embryo contact and focal adhesions during maternal recognition of pregnancy. PLoS One 2019;14 e0213322.

[6] Daels PF, Hughes JP. Fertility control using intrauterine devices: an alternative for population control in wild horses. Theriogenology 1995;44:629-39.

[7] Argo CM, Turnbull EB. The effect of intra-uterine devices on the reproductive physiology and behavior of pony mares. Vet J 2010;186:39-46.

461 [8] Klein V, Müller K, Schoon HA, Reilas T, Rivera del Alamo MM, Katila T. Effects of
462 intrauterine devices in mares: A histomorphological and immunohistochemical
463 evaluation of the endometrium. Reprod Domest Anim 2016;51:98-104.
464 [9] Piras C, Guo Y, Soggiu A, Chanrot M, Greco V, Urbani A, Charpigny G, et al.
465 Changes in protein expression profiles in bovine endometrial epithelial cells
466 exposed to E. coli LPS challenge. Mol Biosyst 2017;13:392-405.
467 [10] Bastos HBA, Martínez MN, Camozzato GC, Estradé MJ, Barros E, Vital CE, et al.
468 Proteomic profile of histotroph during early embryo development in mares.
469 Theriogenology 2019;125:224-35.
470 [11] Arentz G, Weiland F, Oehler MK, Hoffmann P. State of the art of 2D DIGE.
471 Proteomics-Clinical Applications 2015;9:277-288.
472 [12] Portus BJ, Reilas T, Katila T. Effect of seminal plasma on uterine inflammation,
473 contractility and pregnancy rates in mares. Equine Vet J 2005;37:515-9.
474 [13] Reilas T, Katila T. Proteins and enzymes in uterine lavage fluid of postpartum and
475 nonparturient mares. Reprod Domest Anim 2002;37:261-8.
476 [14] Piras C, Soggiu A, Greco V, Martino PA, Del Chierico F, Putignani L. Urbani A,
477 Nally J, Bonizzi L. Roncada P. Mechanisms of antibiotic resistance of
478 enrofloxacin in uropathogenic *Escherichia coli* in dog. J Proteom 2015;127:365-
479 76.
480 [15] Ünlü M, Morgan ME, Minden JS. Difference gel electrophoresis: a single gel method
481 for detecting changes in protein extracts. Electrophoresis 1997;18:2071-7.
482 [16] O'Connell KL, Stults J. Identification of mouse liver proteins on two-dimensional
483 electrophoresis gels by matrix-assisted laser desorption/ionization mass
484 spectrometry of in situ enzymatic digests. Electrophoresis 1997;18:349-59.

485 [17] Shevchenko A, Jensen ON, Podtelejnikov AV, Sagliocco F, Wilm M, Vorm O, et al.
486 Linking genome and proteome by mass spectrometry: large-scale identification of
487 yeast proteins from two dimensional gels. Proc Natl Acad Sci USA
488 1996;93:14440-5.
489 [18] Jensen ON, Larsen MR, Roepstorff P. Mass spectrometric identification and
490 microcharacterization of proteins from electrophoretic gels: Strategies and
491 applications. Proteins 1998;Suppl 2:74-89.
492 [19] Laemmli UK. Cleavage of structural proteins during the assembly of the head of
493 bacteriophage T4. Nature 1970;227:680-5.
494 [20] Pathan M, Keerthikumar S, Chisanga D, Alessandro R, Ang CS, Askenase P, et al.
495 A novel community driven software for functional enrichment analysis of
496 extracellular vesicles data. J Extracell Vesicles 2017;26:1321455.
497 [21] Smits K, Willems S, Van Steendam K, Van De Velde M, De Lange V, Ververs C, et
498 al. Proteins involved in embryo-maternal interaction around the signaling of
499 maternal recognition of pregnancy in the horse. Sci Rep 2018;8:5249.
500 [22] Yoon SJ, Koo DB, Park JS, Choi KH, Han YM, Lee KA. Role of cytosolic malate
501 dehydrogenase in oocyte maturation. Fertil Steril 2006;86:1129-36.
502 [23] Breininger E, Vecchi Galenda BE, Alvarez GM, Gutnisky C, Cetica PD.
503 Phosphofructokinase and malate dehydrogenase participate in the in vitro
504 maturation of porcine oocytes. Reprod Domest Anim 2014;49:1068-73.
505 [24] Dimaano C, Jones CB, Hanono A, Curtiss M, Babst M. Ist1 regulates Vps4
506 localization and assembly. Mol Biol Cell 2008;19:465-74.
507 [25] Rue SM, Mattei S, Saksena S, Emr SD. Novel Ist1-Did2 complex functions at a late
508 step in multivesicular sorting. Mol Biol Cell 2008;19:475-84.

509 [26] Bajorek M, Morita E, Skalicky JJ, Morham SG, Babst M, Sundquist WI.
510 Biochemical analyses of human IST1 and its function in cytokinesis. Mol Biol
511 Cell 2009;20:1360-73.
512 [27] Duester G. Retinoic acid synthesis and signaling during early organogenesis. Cell
513 2008;134:921-31.
514 [28] Avantaggiato V, Acampora D, Tuorto F, Simeone A. Retinoic acid induces stage-
515 specific repatterning of the rostral central nervous system. Dev Bio 1996;175:347-
516 57.
517 [29] Gale E, Zile M, Maden M. Hindbrain specification in the retinoid-deficient quail.
518 Mech Dev 1999;89:43-54.
519 [30] White JC, Highland M, Kaiser M, Clagett-Dame M. Vitamin A deficiency results in
520 the dose-dependent acquisition of anterior character and shortening of the caudal
521 hindbrain of the rat embryo. Dev Biol 2000;220:263-84.
522 [31] Nordling E, Jornvall H, Persson B. Medium-chain dehydrogenases/reductases
523 (MDR). Family characterization including genome comparisons and active site
524 modeling. Eur J Biochem 2002;269:267-76.
525 [32] Yokomizo T, Izumi T, Shimizu T. Leukotriene B_4: Metabolism and signal
526 transduction. Arch Biochem Biophys 2001;15:231-41.
527 [33] Lee EKS, Gillrie MR, Li L, Arnason JW, Kim JH, Babes L, et al. Leukotriene B4-
528 mediated neutrophil recruitment causes pulmonary capillaritis during lethal fungal
529 sepsis. Cell Host Microbe 2018;23:121-33.
530 [34] Dekel N, Gnainsky Y, Granot K, Mor G. Review article: inflammation and
531 implantation. Am J Reprod Immunol 2010;63:17-21.

[35] Chavan AR, Griffith OW, Wagner GP. The inflammation paradox in the evolution of mammalian pregnancy: turning a foe into a friend. Curr Opin Genet Dev 2017;47:24-32.

[36] Oliani SM, Paul-Clark MJ, Christian HC, Flower RJ, Perretti M. Neutrophil interaction with inflamed postcapillary venule endothelium alters annexin 1 expression. Am J Pathol 2001;158:603-15.

[37] Jalali BM, Bogacki M, Dietrich M, Likszo P, Wasielak M. Proteomic analysis of porcine endometrial tissue during peri-implantation period reveals altered protein abundance. J Proteomics 2015;125:76-88.

[38] Romero JJ, Liebig BE, Broeckling CD, Prenni JE, Hansen TR. Pregnancy-induced changes in metabolome and proteome in ovine uterine flushings. Biol Reprod 2017;97:273-87.

[39] Forde N, Carter F, Spencer TE, Bazer FW, Sandra O, Mansouri-Attia N, et al. Conceptus-induced changes in the endometrial transcriptome: How soon does the cow know she is pregnant? Biol Reprod 2011;85:144-56.

[40] Perretti M, D'Acquisto F. Annexin A1 and glucocorticoids as effectors of the resolution of inflammation. Nat Rev Immunol 2009;9:62-70.

[41] Parente L, Solito E. Annexin 1: more than an anti-phospholipase protein. Inflamm Res 2004;53:125-32.

[42] Collard F, Collet JF, Gerin I, Veiga-da-Cunha M, Van Schaftingen E. Identification of the cDNA encoding human 6-phosphogluconolactonase, the enzyme catalyzing the second step of the pentose phosphate pathway. FEBS Letters 1999;459:223-6.

[43] Gardner DK, Harvey AJ. Blastocyst metabolism. Reprod Fertil Dev 2015;27:638-54.

556 [44] Liu X, Lin CY, Lei M, Yan S, Zhou T, Erikson RL. CCT chaperonin complex is
557 required for the biogenesis of functional Plk1. Mol Cell Biol 2005;25:4993-5010.
558 [45] Zebol JR, Hewitt NM, Moretti PA, Lynn HE, Lake JA, Li P, et al. The CCT/TRiC
559 chaperonin is required for maturation of sphingosine kinase 1. Int J Biochem
560 Cell Biol 2009;41:822-7.
561 [46] Granthman J, Brackley KI, Willison KR. Substantial CCT activity is required for
562 cell cycle progression and cytoskeletal organization in mammalian cells. Exp Cell
563 Res 2006;312:2309-24.
564 [47] Pejanovic N, Hochrainer K, Liu T, Aerne BL, Soares MP, Anrather J. Regulation of
565 nuclear factor κB (NF-κB) transcriptional activity via p65 acetylation by the
566 chaperonin containing TCP1 (CCT). Plos One 2012;7:e42020.
567 [48] Hannan NJ, Stoikos CJ, Stephens AN, Salamonsen LA. Depletion of high-abundance
568 serum proteins from human uterine lavages enhances detection of lower-
569 abundance proteins. J Proteome Res 2009;8:1099-103.
570 [49] Borthwick JM, Charnok-Jones DS, Tom BD, Hull ML, Teirney R, Phillips SC, Smith
571 SK. Determination of the transcript profile of human endometrium. Mol Hum
572 Reprod 2003;9:19-33.
573 [50] Ponnampalam AP, Weston GC, Trajstman AC, Susil B, Rogers PA. Molecular
574 classification of human endometrial cycle stages by transcriptional profiling. Mol
575 Hum Reprod 2004;10:879-93.
576 [51] Arlas TR, Wolf CA, Petrucci BPL, Estanislau JF, Gregory RM, Jobim MIM, Mattos
577 RC. Proteomics of endometrial fluid after dexamethasone treatment in mares
578 susceptible to endometritis. Theriogenology 2015;84:617-23.
579 [52] Zavy MT, Sharp DC, Bazer FW, Fazleabas A, Sessions F, Roberts RM. Identification
580 of stage-specific and hormonally induced polypeptides in the uterine protein

secretions of the mare during the oestrous cycle and pregnancy. J Reprod Fertil 1982;64:199-207.

[53] Ginther OJ, Gastal EL, Gastal MO, Utt MD, Beg MA. Luteal blood flow and progesterone production in mares. Anim Reprod Sci 2007;99:213-20.

[54] Ginther OJ, Castro T, Baldrighi JM, Wolf CA, Santos VG. Defective secretion of prostaglandin F2a during development of idiopathic persistent corpus luteum in mares. Domest Anim Endocrinol 2016;55:60-5.

590 **Figure legends**

591 **Fig. 1.** Experimental protocol for collecting uterine lavage fluid for two-dimensional
592 difference gel electrophoresis (2D-DIGE). AI: artificial insemination; IUD: intrauterine
593 device; US: ultrasound examination; P4: progesterone; AI-P: pregnant mares; AI-N: non-
594 pregnant mares; PGFM: 15-ketodihydro-$PGF_{2\alpha}$; COX-2: cyclooxygenase 2; IUD-P:
595 prolonged luteal phase; IUD-N: normal luteal phase.

596

597 **Fig. 2.** A representative 2D-DIGE gel image of the endometrial secretome of mares.
598 Proteins with different abundance are marked with red circles. 1: non-identified protein;
599 2: T-complex protein (TCP1); 5: hemoglobin; 8: 6-phosphogluconolactonase (6PGL); 11:
600 increased sodium tolerance 1 (IST1); 12: prostaglandin reductase 1 (PTGR1); 13:
601 aldehyde dehydrogenase 1A1 (ALDH1A1); 16: malate dehydrogenase 1 (MDH1); 17:
602 annexin A1 (ANXA1).

603

604 **Fig. 3.** Graphical representation of the standardized log abundance of the identified
605 proteins in the endometrial secretome from each group of mares. TCP1: T-complex
606 protein 1; PTGR1: prostaglandin reductase 1; 6PGL: 6-phosphogluconolactonase MDH1:
607 malate dehydrogenase 1; IST1: increased sodium tolerance 1; ANXA1: annexin A1;
608 ALDH1A1: aldehyde dehydrogenase 1A1. AI-P: pregnant mares; AI-N: non-pregnant
609 mares; IUD-N: device mares with normal luteal phase; IUD-P: device mares with
610 prolonged luteal phase.

611

612 **Fig. 4.** Western blotting confirmation of 2D-DIGE results for proteins 6PGL, IST1,
613 PTGR1, ALDH1A, MDH1 and Annexin A1. A 20-µl aliquot of pooled samples were
614 used for each verification. AI-P: pregnant mares; AI-N: non-pregnant mares; IUD-P:

615 device mares with prolonged luteal phase; IUD-N: device mares with normal luteal
616 phase.
617
618 **Fig. 5.** Gene ontology (GO) classification of the identified proteins. Proteins were
619 grouped into three main GO categories: biological process (BP), molecular function (MF)
620 and cellular component (CC). Bonferroni corrected p-values were transformed by log10.
621
622 **Supplementary Fig. S1.** Workflow for the 2D-DIGE analysis of uterine lavage.
623 Extracted proteins were labelled with fluorescent dyes according to the table and proteins
624 were separated by 2D-PAGE. The gel images were analyzed and statistically assessed
625 with DeCyder software. Spots of interest were cut from the gels and proteins were
626 identified with mass spectrometry. AI-P: pregnant mares; AI-N: non-pregnant mares;
627 IUD-P: device mares with prolonged luteal phase; IUD-N: device mares
628 with normal luteal phase.
629
630

Table 1. Proteins identified by LC-MS/MS following 2D-DIGE analysis.

Spot no	Identified protein	Accession number	Theoretical pI/MW (Da)	Matched peptides	Sequence coverage (%)	MASCOT score
2	TCP1	Q4R5J0	5.5/59.7	4	8	43
8	6PGL	OP5RR6	5.6/27.5	6	27.1	38
11	IST1	Q3ZBV1	5.23/39.7	1	2.4	41
12	PTGR1	Q29073	8.39/35.7	3	10.3	52
13	ALHD1A1	P15437	6.43/54.7	1	2.2	60
16	MDH1	P40925	6.91/36.4	4	11.9	93
17	ANXA1	Q8HZM6	5.67/38.7	6	16.7	111

pI: isoelectric point; MW: molecular weight; TCP1: T-complex protein 1; 6PGL: 6-phosphogluconolactonase; IST1: increased sodium tolerance 1; PTGR1: prostaglandin reductase 1; ALDH1A1: aldehyde dehydrogenase 1A1; MDH1: malate dehydrogenase 1; ANXA1: annexin A1.

638 **Table 2.** Average ratios of 2D-DIGE analyses between pregnant mares (AI-P) and either
639 non-pregnant (AI-N) or device (IUD) mares.
640

Spot nº	Identified protein	AI-N vs AI-P	IUD-N vs AI-P	IUD-P vs AI-P
		Average ratio, one-way ANOVA (p-value)		
2	TCP-1	2.46 (0.0064)	1.29 (0.016)	1.88 (0.0025)
8	6PGL	2.08 (0.0064)	3.60 (0.00036)	1.68 (0.27)
11	IST1	-4.21 (0.015)	-1.69 (0.35)	-3.51 (0.037)
12	PTGR1	-2.49 (0.03)	-2.05 (0.11)	-1.27 (0.6)
13	ALDH1A1	-4.31 (0.023)	-1.96 (0.26)	-4.07 (0.33)
16	MDH1	-3.376 (0.021)	-1.85 (0.21)	-3.09 (0.029)
17	ANXA1	1.40 (0.041)	1.67 (0.012)	1.84 (0.0014)

641

642 AI-P: pregnant mares; AI-N: non-pregnant mares IUD-N: device mares with normal
643 luteal phase; IUD-P: device mares with prolonged luteal phase; TCP1: T-complex protein
644 1; 6PGL: 6-phosphogluconolactonase; IST1: increased sodium tolerance 1; PTGR1:
645 prostaglandin reductase 1; ALDH1A1: aldehyde dehydrogenase 1A1; MDH1: malate
646 dehydrogenase 1; ANXA1: annexin A1.

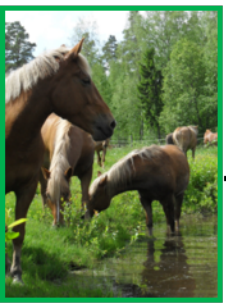

n=16

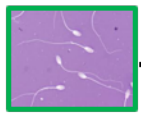

Day -1 (24 h after hCG)

AI

n = 8

Day 3 post ovulation

IUD

n = 8

Day 14 & 15
Ultrasound and serum progesterone (P4)

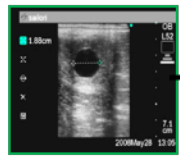

AI-N (n = 4)
Non-pregnant group

AI-P (n = 4)
Pregnant group

IUD-N (n = 4)
Normal cycle
Low P4

IUD-P (n = 4)
Prolonged luteal phase
High P4

Day 15
Uterine fluid collection by low-volume lavage

Protein extraction and labelling

Gel	Cy2	Cy3	Cy5
1	Internal Std	AI-P 1	IUD-N 1
2	Internal Std	IUD-P 1	AI-N 1
3	Internal Std	AI-N 2	IUD-N 2
4	Internal Std	AI-N 3	IUD-N 3
5	Internal Std	IUD-P 2	IUD-N 4
6	Internal Std	AI-N 4	AI-P 2
7	Internal Std	AI-P 3	AI-P 4
8	Internal Std	IUD-P 3	IUD-P 4

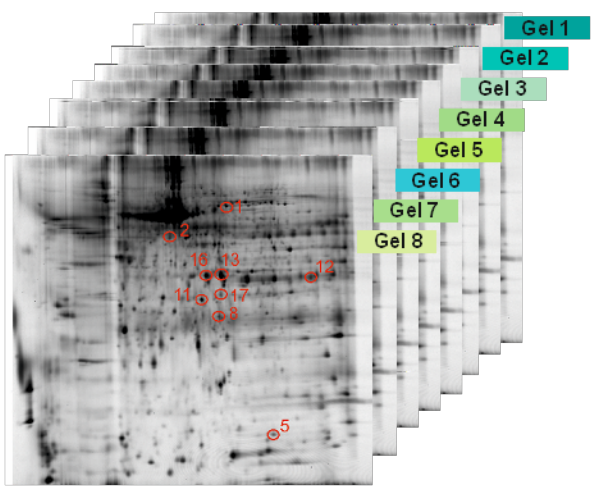

2: TCP1; **5**: hemoglobin; **8**: 6-PGL; **11**: IST1; **12**: PTGR1; **13**: ALDH1A1; **16**: MDH1; **17**: ANXA1.

AI-P (N=4)

AI-N (n=4)

IUD-P (N=4)

IUD-N (N=4)

Protein extraction and labelling

Gel	Cy2	Cy3	Cy5
1	Internal Std	AI-P 1	IUD-N 1
2	Internal Std	IUD-P 1	AI-N 1
3	Internal Std	AI-N 2	IUD-N 2
4	Internal Std	AI-N 3	IUD-N 3
5	Internal Std	IUD-P 2	IUD-N 4
6	Internal Std	AI-N 4	AI-P 2
7	Internal Std	AI-P 3	AI-P 4
8	Internal Std	IUD-P 3	IUD-P 4

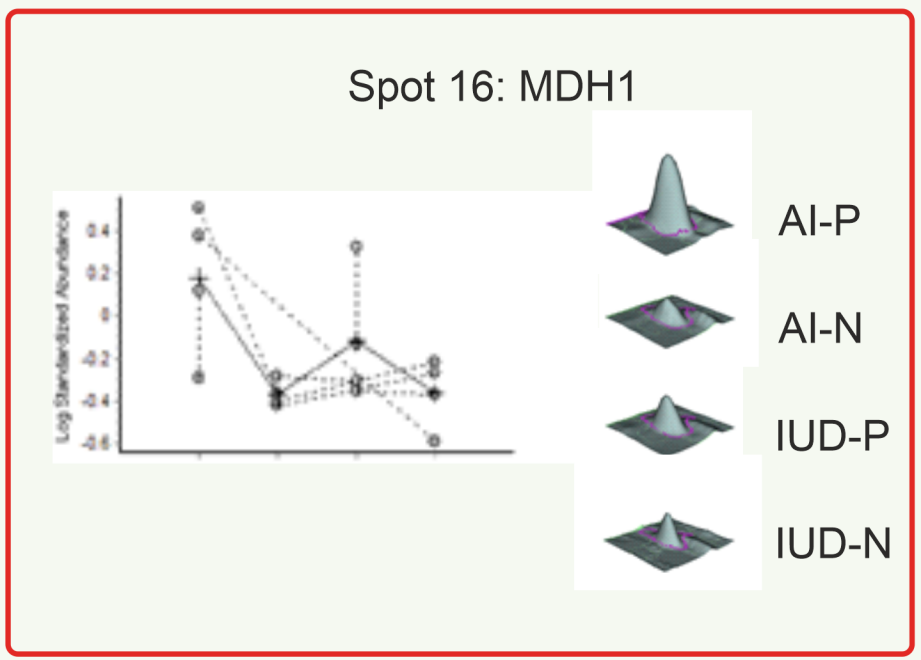

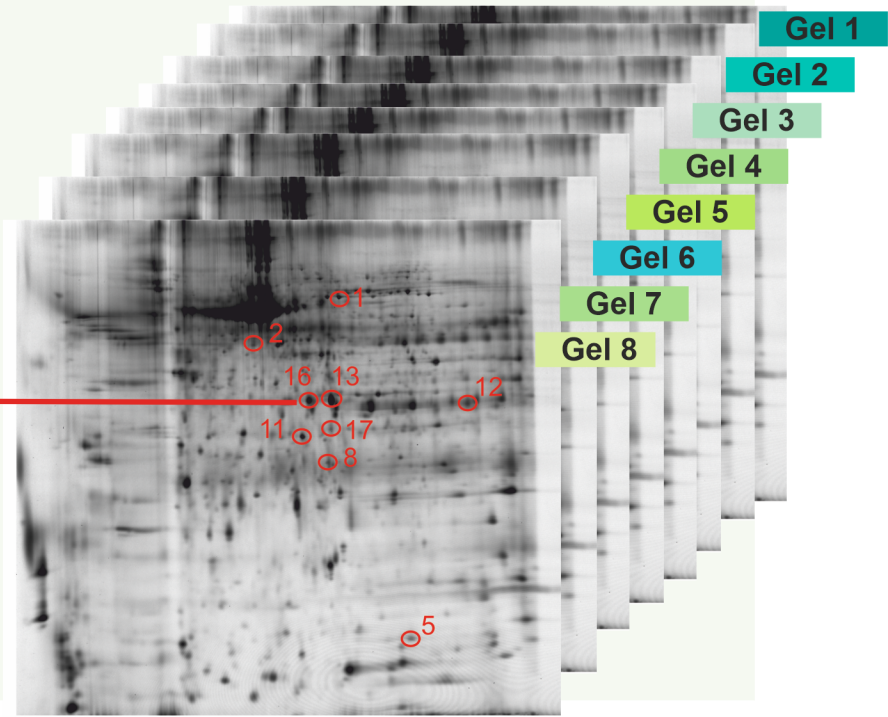

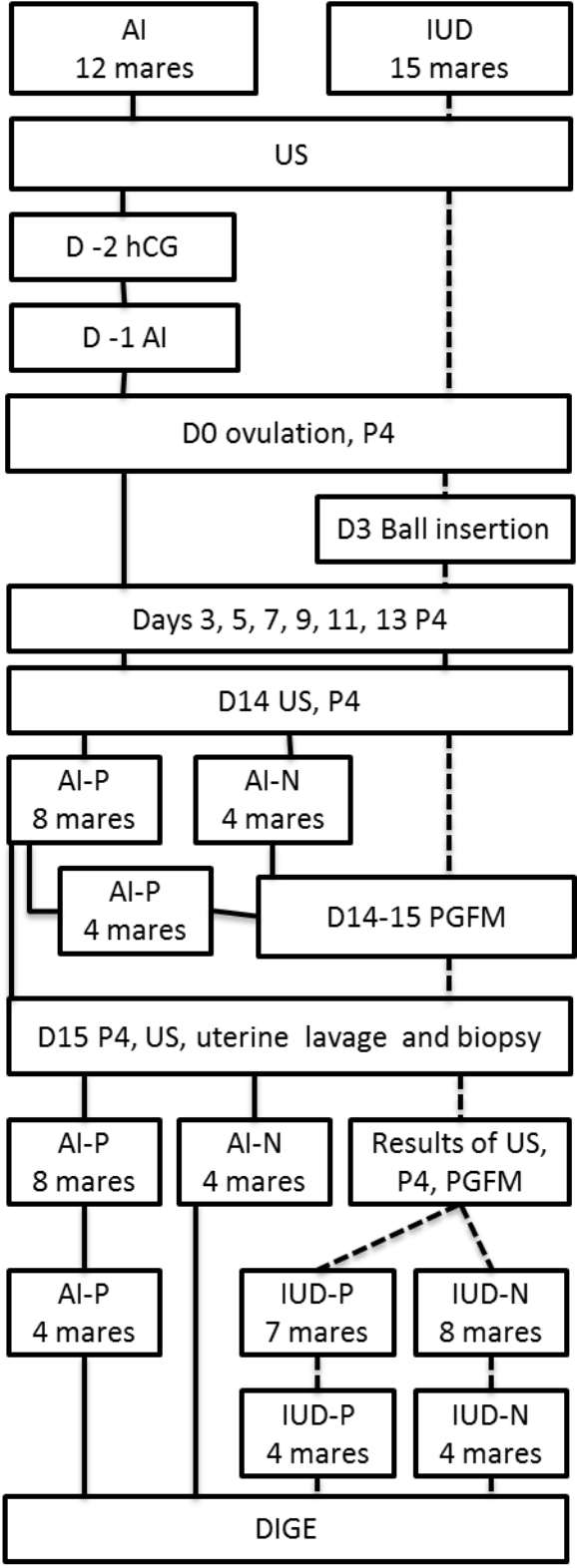
AI
12 mares
IUD
15 mares
US
D -2 hCG
D -1 AI
D0 ovulation, P4
D3 Ball insertion
Days 3, 5, 7, 9, 11, 13 P4
D14 US, P4
AI-P
8 mares
AI-N
4 mares
AI-P
4 mares
D14-15 PGFM
D15 P4, US, uterine lavage and biopsy
AI-P
8 mares
AI-N
4 mares
Results of US, P4, PGFM
AI-P
4 mares
IUD-P
7 mares
IUD-N
8 mares
IUD-P
4 mares
IUD-N
4 mares
DIGE

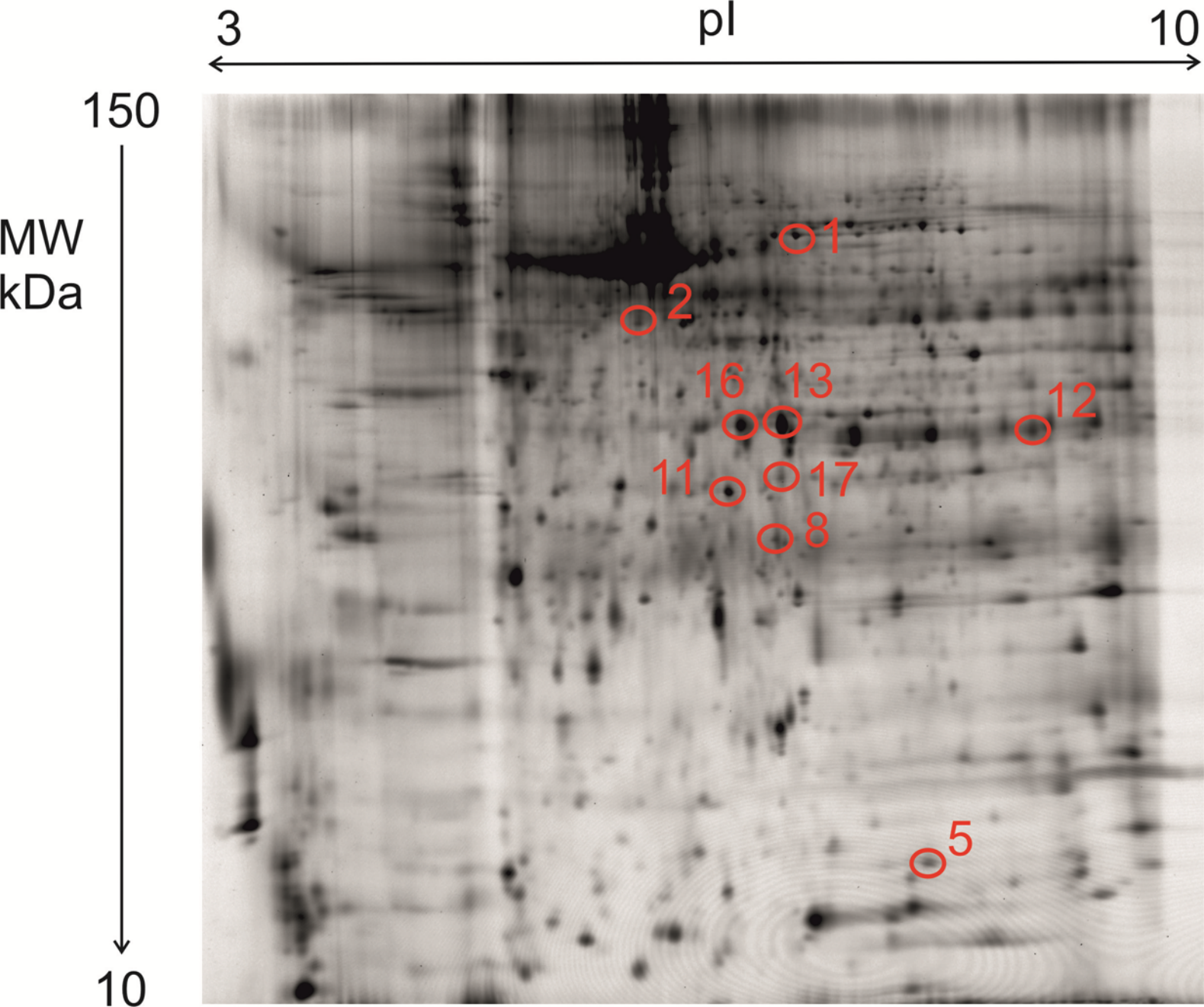
3
pI
10
150
MW
kDa
10
1
2
16
13
12
11
17
8
5

TCP1

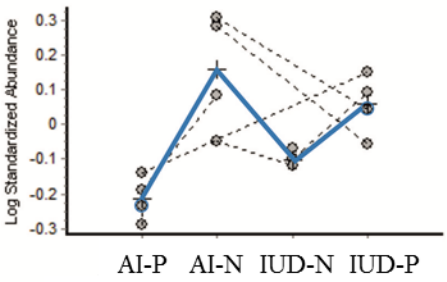

PTGR1

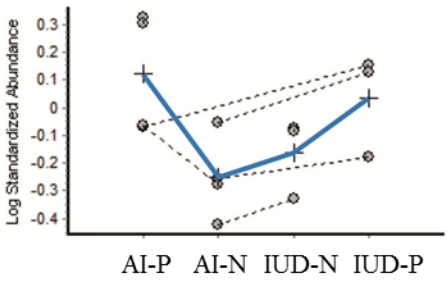

6-PGL

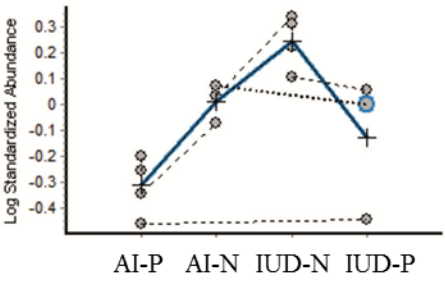

MDH1

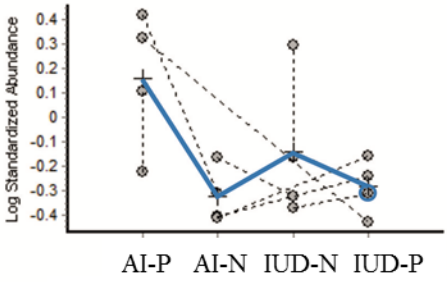

IST1

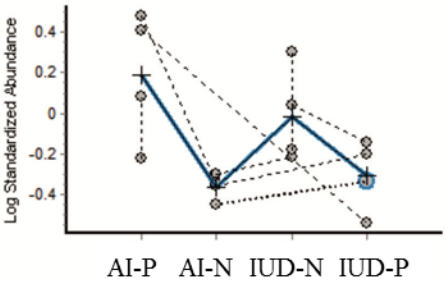

ANXA1

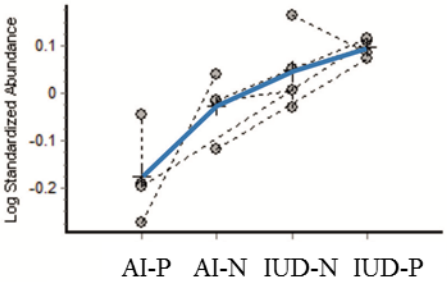

ALDH1A1

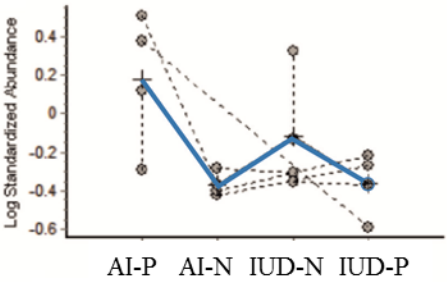

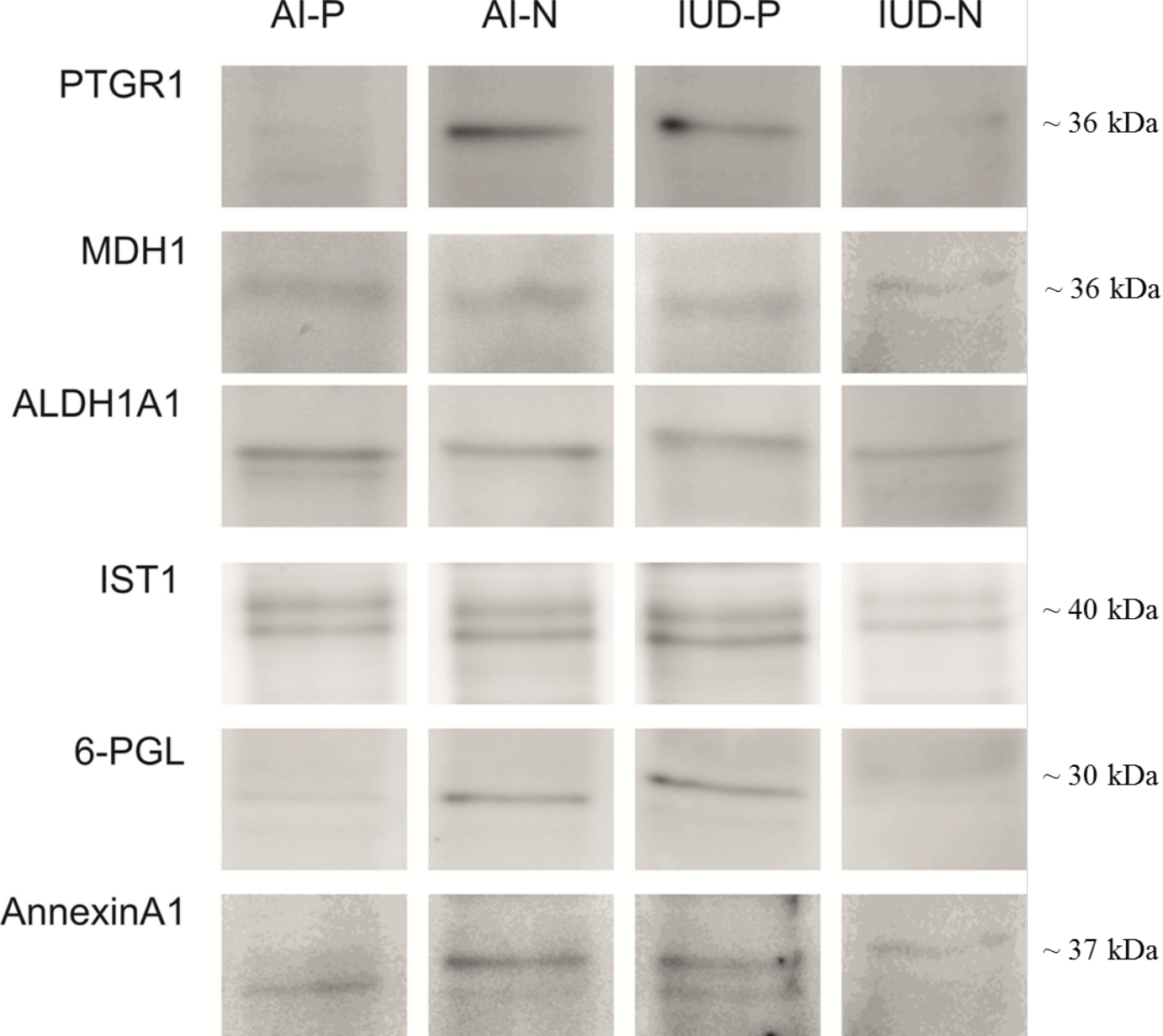
AI-P
AI-N
IUD-P
IUD-N
PTGR1
~ 36 kDa
MDH1
~ 36 kDa
ALDH1A1
IST1
~ 40 kDa
6-PGL
~ 30 kDa
AnnexinA1
~ 37 kDa

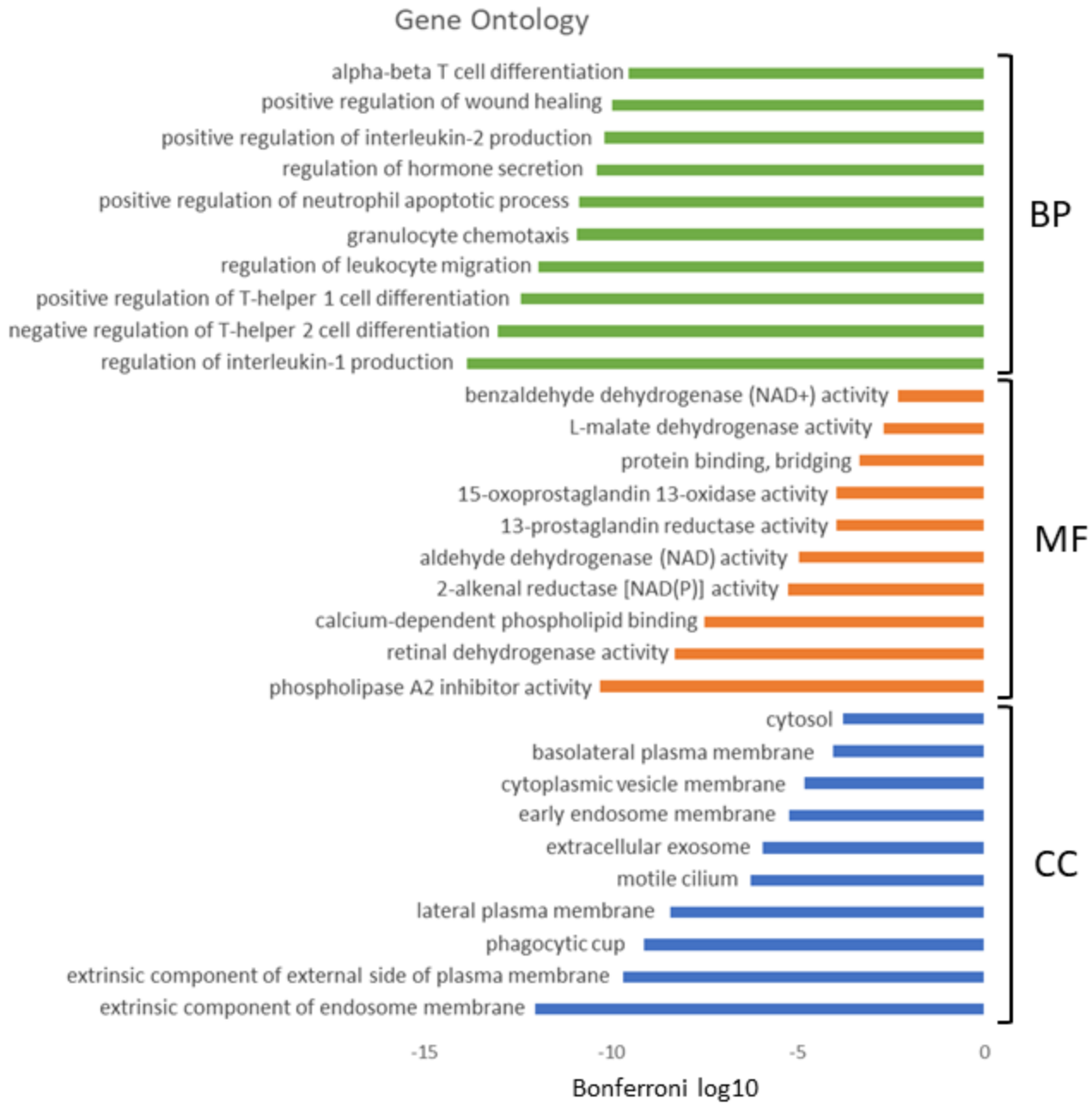
Gene Ontology
alpha-beta T cell differentiation
positive regulation of wound healing
positive regulation of interleukin-2 production
regulation of hormone secretion
positive regulation of neutrophil apoptotic process
granulocyte chemotaxis
regulation of leukocyte migration
positive regulation of T-helper 1 cell differentiation
negative regulation of T-helper 2 cell differentiation
regulation of interleukin-1 production
BP
benzaldehyde dehydrogenase (NAD+) activity
L-malate dehydrogenase activity
protein binding, bridging
15-oxoprostaglandin 13-oxidase activity
13-prostaglandin reductase activity
aldehyde dehydrogenase (NAD) activity
2-alkenal reductase [NAD(P)] activity
calcium-dependent phospholipid binding
retinal dehydrogenase activity
phospholipase A2 inhibitor activity
MF
cytosol
basolateral plasma membrane
cytoplasmic vesicle membrane
early endosome membrane
extracellular exosome
motile cilium
lateral plasma membrane
phagocytic cup
extrinsic component of external side of plasma membrane
extrinsic component of endosome membrane
CC
-15
-10
-5
0
Bonferroni log10